

T cell Bispecific Antibodies in Node-Positive Breast Cancer: Novel Therapeutic Avenue for MHC class I Loss Variants.**Authors:**

M. Messaoudene^{1,2}, T.P. Mourikis³, J. Michels^{1,4,5}, Y. Fu¹, M. Bonvalet^{1,2}, M. Lacroix-Trikki^{1,7}, B. Routy^{1,6}, A. Fluckiger^{1,2,7}, S. Rusakiewicz⁹, M.P. Roberti^{1,2,7}, S. Cotteret¹, C. Flament^{1,2,7}, V. Poirier-Colame^{1,2,7}, N. Jacquelot^{1,2,4}, F. Ghiringhelli¹⁰, A. Caignard¹¹, A.M.M. Eggermont¹, G. Kroemer^{1,4,12}, A. Marabelle^{1,2,4,13}, M. Arnedos^{1,5}, C. Vicier¹⁴, S. Dogan^{1,5,14}, F. Jaulin^{1,5,14}, S-J. Sammut¹⁵, W. Cope^{15,16}, C. Caldas¹⁵, S. Delaloge^{1,5,#}, N. McGranahan^{3,#}, F. André^{1,5,14,#}, and L. Zitvogel^{1,2,4,7,#,*}.

Affiliations:

¹*Gustave Roussy Cancer Campus (GRCC), Villejuif, France.*

²*National Institute of Health and Medical Research (INSERM) U1015, Villejuif, France.*

³*Cancer Research UK Lung Cancer Centre of Excellence, University College London Cancer Institute, London, UK.*

⁴*University Paris-Sud, University Paris-Saclay, Gustave Roussy Cancer Campus (GRCC), Villejuif, France.*

⁵*Department of Medical Oncology, Gustave Roussy, Villejuif, France.*

⁶*Université de Montréal Hospital Research Centre (CRCHUM), Onco-hematology department, Montreal University Hospital Center (CHUM), Montréal, Québec, Canada.*

⁷*Center of Clinical Investigations in Biotherapies of Cancer (CICBT) 1428, Villejuif, France.*

⁸*Department of Pathology, Gustave Roussy, Villejuif, France.*

⁹*Center of experimental therapeutics (CET), Department of Oncology, Lausanne University Hospital, CHUV, Lausanne, Switzerland.*

¹⁰*Georges-François Leclerc center, Medical Oncology, Dijon, France.*

¹¹*INSERM U1160, University Institute for Haematology, Saint Louis hospital, Paris, France.*

¹²*Cell Biology and Metabolomics Platforms, Gustave Roussy Cancer Campus, Cordeliers research center, INSERM, U1138, Université Paris Descartes, Sorbonne Paris Cité, Paris, France; Université Pierre et Marie Curie, Paris, France; Pôle de Biologie, Européen Georges Pompidou Hospital, AP-HP, Paris, France.*

¹³*Gustave Roussy Cancer Campus (GRCC), Drug Development Department (DITEP), Villejuif, France.*

¹⁴*Gustave Roussy Cancer Campus (GRCC), INSERM U981, Villejuif, France.*

¹⁵*Cancer Research UK Cambridge Institute and Department of Oncology, University of Cambridge, Cambridge, UK.*

¹⁶*Cancer Research UK Cancer Centre and National Institute for Health Research Cambridge Biomedical Research Centre, Cambridge University Hospitals NHS Foundation Trust, Cambridge, UK*

Co-last authors

* *Corresponding author.*

Prof. Laurence Zitvogel,
Gustave Roussy institut,
114 rue Edouard Vaillant, 94805 VILLEJUIF Cedex, France
E-mail: Laurence.ZITVOGEL@gustaveroussy.fr
Phone: +33 1 42 11 50 41
Fax: +33 1 42 11 60 94

Abbreviations: ATP: Adenosine Triphosphate, BC: Breast Cancer, CAFs: Cancer-Associated Fibroblasts, CAR T cells: Chimeric Antigen Receptor T cells, CEACAM5: Carcinoembryonic Antigen-Related Cell Adhesion Molecule 5, CEACAM5-T: CD3-CEACAM5 bispecific antibody, CGH: Comparative genomic hybridisation, CRT: Calreticulin, CTL : Cytotoxic T Lymphocytes, Ctrl: Control, CXCL10: C-X-C motif chemokine 10, DC: Dendritic Cells, DCIS: Ductal Carcinoma, EBC: Early Breast Cancer, EpCAM: Epithelial Cell Adhesion Molecule, ER : Estrogen Receptor, ERBB2: Erb-B2 Receptor Tyrosine Kinase 2, FAP: Fibroblast Activation Protein, Foxp3 : Forkhead box protein P3, FPR1: Formyl Peptide Receptor 1, GrzB: Granzyme B, HER2: Human Epidermal growth factor Receptor 2, HER2-T: CD3-HER2 bispecific antibody, HER2-UNT: untargeted HER2-UNT Antibody, HLA : Human Leukocyte Antigen, HLA LOH: HLA loss of heterozygosity, HMGB1: High Mobility Group B1, HR: Hormone Receptor, HT: Healthy Tissues, ICD: Immunogenic Cell Death, IDC: invasive DC, IFN : Interferon, mAB: Monoclonal Antibodies, MAPK: Mitogen-Activated Protein Kinase, MHC : Major Histocompatibility Complex, mLN : Metastatic Lymph Nodes, NFATC1: Nuclear Factor of Activated T-Cells 1, NF- κ B1: Nuclear Factor-Kappa B1, NK: Natural Killer, NR: Resistance, PD-1: Programmed cell Death-1, PD-L1: Programmed Death-Ligand 1, R: Responsiveness, RNASeq : RNA Sequencing, SEM: Standard Error of the Mean, SLN: Sentinel Lymph Node, TCB : T cell bispecific antibodies, TCGA: The Cancer Genome Atlas, TCR: T Cell Receptor, TILs : Tumor-Infiltrating Lymphocytes, Tim3 : T-cell Immunoglobulin and Mucin-domain-3, TLR4: Toll-Like Receptor, TNBC: Triple Negative Breast Cancer.

Abstract

Background: Tumor-infiltrating lymphocytes (TILs) represent a prognostic factor for survival in primary breast cancers (BC). Nonetheless, neoepitope load and TILs cytolytic activity are modest in BC, compromising the efficacy of immune-activating antibodies, which do not yet compete against immunogenic chemotherapy.

Patients and methods: We analyzed by functional flow cytometry the immune dynamics of primary and metastatic axillary nodes (mLN) in early breast cancers after exposure to T cell bispecific antibodies (TCB) bridging CD3 ϵ and HER2 or CEACAM5, before and after chemotherapy. HLA class I loss was assessed by whole exome sequencing and immunohistochemistry. 100 primary BC, 64 surrounding “healthy tissue” (HT) and 24 mLN related-parameters were analyzed.

Results: HLA loss of heterozygosity was observed in early BC, at a clonal and subclonal level and was associated with regulatory T cells and Tim3 expression restraining the immuno-stimulatory effects of neoadjuvant chemotherapy. TCB bridging CD3 ϵ and HER2 or CEACAM5 could bypass MHC class I loss, partially rescuing T cell functions in mLN.

Conclusion: TCB should be developed in BC to circumvent low MHC/peptide complexes.

Key words

Breast cancer, Tumor-infiltrating lymphocytes (TILs), T cell bispecific antibodies (TCB), HER2, CEACAM5, HLA loss.

Key message

In this original article, the authors showed that HLA loss of heterozygosity is observed in early Breast Cancer, and is associated with Treg cells and Tim3 expression restraining the immuno-stimulatory effects of chemotherapy. T cell bispecific antibodies (TCB) bridging CD3 ϵ and HER2 or CEACAM5 could bypass HLA loss, partially restoring T cell functions in axillary lymph nodes.

Introduction

Like colon carcinoma, breast cancers (BC) have been one of the first anatomopathological entities to be described as “immune infiltrated“ but paradoxically turned out to be relatively ”immunoresistant“. First, distinct molecular subtypes of BC are intrinsically immunogenic in that some immunological metrics (1) harbor independent prognostic and predictive values for overall or progression-free survival during therapies. Pathologic analysis can reveal not only the numbers of TILs, the presence of follicular CD4⁺ T cells but also the pattern of infiltration, including tertiary lymphoid organs, relevant mainly in triple negative breast cancer (TNBC) and human epidermal growth factor receptor 2 (HER2)⁺ BC (2). TILs density is also a predictor of pathological complete response following neoadjuvant chemotherapy (3). Secondly, conventional therapies against BC play a major role in activating the immune system by inducing immunogenic cell death (ICD) (4,5). Third, despite several tumor-associated antigens described as immunogenic in BC vaccination trials, they were not protective against disease progression (6)(7). Hence, in contrast to other malignancies, there have been few clinical trials using programmed death 1 (PD-1) or -ligand-1 (PD-L1) monoclonal antibodies (mAb) which achieves objective response rates in the 12-19% range when administered alone (8), or combined with taxanes in first-line metastatic TNBC (9). Hence, the lack of a clinically relevant immuno-dominant T cell receptor (TCR) repertoire capable of expanding post-chemotherapy remains a challenging issue. The current strategies to circumvent this issue are chimeric antigen receptor redirected T cells and T cell bispecific antibodies (TCB). TCB redirect T cells to tumor cells, by connecting a T cell via CD3ε to a tumor-specific antigen on the surface e.g. HER2 or CEACAM5 (10)(11). This induces the formation of a transient cytolytic synapse between the cytotoxic T cell and the tumor cell resulting in T-cell activation, proliferation, and serial lysis of tumor cells. TCB-mediated T-cell activation does not rely on the presence of MHC class I molecules and tumor-specific peptide antigens (10). We have previously described novel heterodimeric 2+1 T cell bispecific antibodies based on a human IgG1 backbone using an Fc-region without residual FcγR binding (12)(13). Here, we show that i) immunogenic chemotherapy failed to switch on effector T cells in metastatic lymph nodes (mLN) of BC where Tim3 and Treg dominated the phenotype, ii) high prevalence of HLA class I loss of heterozygosity in tumor cells

reaching axillary LN in paired specimens could explain TILs inactivation, iii) HER2-TCB or CEACAM5-TCB reinstate TILs effector functions in mLN, circumventing MHC class I loss variants.

Materials and methods

Patients and cohorts.

Study approval. Institutional review board approval was granted by the University Paris Saclay and Gustave Roussy/Kremlin Bicêtre for the prospective cohort which was previously described (SAFIR01 (13)). The human study protocols were in accordance with the Declaration of Helsinki principles, and all patients provided informed consent before enrollment in the study.

Prospective cohort of stage I/II BC patients. Tumor infiltrating cells were analyzed prior to chemotherapy (in N=38 patients) or after neoadjuvant chemotherapy (in N=97 patients). A total of 100 primary BC lesions (table S1 and S2), 64 paired “Healthy Tissue” (HT) and 24 dissociated metastatic lymph nodes were analyzed after surgery at diagnosis or post-chemotherapy.

Experimental Design.

Details feature in Supplemental materials. Briefly, BC lumps, mLN and paired surrounding healthy tissues were dissociated and subjected to *ex vivo* assays as previously described (14). The *ex vivo* assay consisted in stimulating the immune cells from 14 primary BC and 21 dissociated mLN with mAbs (T cell bispecific antibodies (TCB) HER2-CD3, CEACAM5-CD3 or controls), anti-FAP-41BBL, and combinations) or cytokines (rIL-2) (Fig. S2) for 2-6 days in 48-well plates as described in the Fig. S2, followed by flow cytometric analysis of T and NK cells and cytokine monitoring in ELISA of culture supernatants. We arbitrarily defined “responding” lesions, those exhibiting > 1.5-fold change over two different controls (medium and untarget-anti-CD3) in 3 independent biological readouts (out of 6 readouts, GrzB or Ki67 positivity on CD4⁺, CD8⁺ T cells or NK cells).

Flow cytometric analyses and cytokine/chemokine monitoring.

TILs from 77 primary BC and 15 mLN were stained with fluorochrome-coupled mAbs (detailed in table S3), incubated for 20 min at 4°C and washed with PBSX1. Cell samples were acquired on a Cyan ADP 9-color (Beckman Coulter) and BD FACS Canto II flow-cytometers with single-stained antibody-capturing beads used for compensation (Compbeads, BD Biosciences). Data were analyzed with Kaluza 1.3 (Beckman). Supernatants from cultured cells were monitored using commercial ELISA (BD Biosciences).

Staining of HER2 and HLA class I.

Immunohistochemistry was performed using HLA-I, mouse anti-human HLA A, B and C mAb (MBL, clone EMR8-5, 0,5µg/ml, 1:750 dilution, on 3µm-thick sections of formalin-fixed, paraffin-embedded breast cancer tissue sections on a Leica Bond RX with their Polymer Refine Detection System. Also refer to Supplementary materials.

HLA class I genes scoring.

A total of 695 metastatic BC from clinical trial SAFIR01 (13) and SAFIR02 from Gustave Roussy (France) and 1080 primary BC from TCGA and METABRIC were included in the analysis. Segments with copy number variants were detected by Comparative genomic hybridisation (CGH) array and the raw data were processed using a R package rCGH (15). Also refer to supplemental materials.

LOHHLA (Loss Of Heterozygosity in Human Leukocyte Antigen) methodology and algorithm.

Copy number inference of HLA alleles was performed using LOHHLA (15) on whole exome sequencing data. For further details refer to Supplemental materials.

Statistics.

Data analyses and graphical representations were performed with Prism 7 (GraphPad, San Diego, CA, USA) and R version 3.4. The nonparametric Mann-Whitney test was used for comparison between primary BC

versus HT or mLN. Correlations between different parameters were assessed by nonparametric Spearman test. *p*-values are two-sided and 95% confidence intervals for the statistic of interest are reported.

Results

Metastatic lymph nodes differ from primary lesions in the dynamics of immune composition in BC.

We investigated the composition of immune infiltrates in early breast cancers (EBC) amenable to surgical resection, either before chemotherapy (“adjuvant” setting) or after conventional anthracycline/taxane-based chemotherapy (“neoadjuvant” setting). Patients baseline characteristics in the adjuvant and neoadjuvant setting are detailed in Table S1 and Table S2, respectively. Flow cytometric analyses of freshly dissociated primary tumors at diagnosis were compared with surrounding “healthy” tissues (HT), revealing several cancer-associated immune hallmarks. Cancerous lesions were enriched in leukocytes (Fig. S1a) in an immunosuppressive contexture. Regulatory T cells defined by CD25^{high}CD127^{low}/CD4⁺ T cells (Fig. S1b, left panel) were accompanied with conventional T cells overexpressing PD-1/PD-L1 (Fig. S1c, left and middle panels) while non-T and non-NK cells (CD3⁻CD56⁻, mostly myeloid and B cells (14)) expressed higher levels of PD-L1 (Fig. S1c, right panel) in tumors. The immune profiles of hormone receptor (HR)⁺, HER2⁺, TNBC did not significantly differ in primary or metastatic lymph nodes (mLN) except for CD25^{high}CD127^{low} CD4⁺ Treg cells that preferentially accumulated in HER2⁺ and TNBC (Fig. S1b right panel, Table S4).

We next examined the immune profiles of tumors subjected to neoadjuvant chemotherapy, mostly represented by locally advanced BC. Surprisingly, the immune microenvironment of mLN appeared different from their primary lesion. First, the proportion of CD8⁺ TILs markedly increased with chemotherapy in primary lesions with a significant rise of the CD8/CD4 ratio but less so in mLN (Fig. 1a left panel, Fig. 1b). Second, the three immune checkpoints (Treg, PD-1, Tim3), hallmarks of T cell activation, were decreased in mLN CD4⁺ TILs compared to primary tumors prior to chemotherapy (Fig. 1c). Third, chemotherapy failed to induce degranulation of CTLs in mLN (Fig. 1a right panel) but did induce

Tim3 expression (superior to that observed in primary lesions) and Treg in CD4⁺ TILs of mLN (Fig. 1c). Altogether, the CD8/CD4 ratio was largely in favor of CD4⁺ T cells despite neoadjuvant chemotherapy in mLN (Fig. 1b). Interestingly, the live CD45⁻ fraction (Fig. 1d) was positively associated with a favorable and higher CD8/CD4 ratio in mLN in the neoadjuvant setting (Fig. 1e).

Immunogenic chemotherapy could switch on effector T cells in primary lesions but failed to do so in metastatic lymph nodes where Tim3 and Treg dominated the scenario.

Immune effects of IgG-based T-cell bispecific antibodies (TCB) in BC

To reinstate resident T cell functions in mLN, we utilized IgG-based T-cell bispecific antibodies (TCB) on freshly dissociated BC (in the previously described *in vitro* assays (14), Fig. S2). The bioactivity of the HER2-CD3 ϵ TCB (HER2-T) was compared to medium alone and untargeted control Ab (Ctrl-T) with rIL-2 (as a positive control) in 3-16 lesions. The results of the functional assays describing the dynamics of the immune profile at Day 1 of co-cultures are summarized in the heat-map presented in Fig. 2a and Supplemental Fig. 3a for tumors handled in adjuvant and neoadjuvant settings, respectively. Briefly, HER2-T triggered degranulation of CD8⁺ and NK TILs (Fig. 2b-c, Fig. S3b-c), their proliferation (Fig. 2d, Fig. S3d) as well as IFN γ cytokine release in T cells (Fig. 2e, Fig. S3e), mainly in mLN in the adjuvant setting. However, HER2-T did not increase TNF α production by T cells nor the inflammatory contexture of BC (Fig. 2a, Fig. S3a). Of note, primary tumor-residing T cells already exposed and responding to chemotherapy failed to further react to HER2-T in most patients, and these reagents also failed to ameliorate the low degranulation and proliferative capacity (Fig. S3b-d) as well as IFN γ cytokine release in tumor T cells (Fig. S3e). Importantly, HER2-T was not efficient at reinstating mLN TILs functions after neoadjuvant chemotherapy, regardless of TCB dose (Fig. S4).

Next, we investigated the CEACAM5-CD3 ϵ T cell bispecific antibody (CEACAM5-T) in about 10 lesions at increasing doses in mLN only in adjuvant settings. Its format incorporates bivalent binding to CEACAM5, a head-to-tail fusion of CEACAM5- and CD3 ϵ -binding Fab domains as well as an engineered Fc region

which completely abolished binding to Fc γ Rs and C1q (16). As observed using the HER2-T, the CEACAM5-T induced T and NK cell effector functions and entry into the cell cycle (Ki67), even at low dosing of TCB (Fig. 3). Interestingly, in 3/5 cases tested, CEACAM5-T turned HER2-T-resistant lesions into positive ones (Fig. S5a-b).

In as much as i) Tim3 and PD-1 were expressed at high levels on CD4⁺ TILs from mLN (Fig. 1), ii) Tim3 and 4-1BBL (CD137L) were upregulated by HER2-T (Fig. S5c-d), iii) Fibroblast Activation Protein (FAP) was expressed on stromal cells in BC (Fig. S5e), we undertook to admix HER2-T with other bispecific antibodies (anti-FAP-4-1BBL and controls) (listed in Fig. S2) to boost T cell functions. In some cases (5 cases out of 12 tested), lesions resistant to HER2-T could respond to anti-FAP-4-1BBL antibodies for proliferation or GrzB and Th1 cytokine release (Fig. S5f-h).

We next analyzed which factors could predict responsiveness in *in vitro* assays to TCB. HER2 and CEACAM5 expression levels by tumor cells allowed to some extent to contrast responding (R) from non-responding (NR) lesions (Fig. S6a-c). Naïve tumors unexposed to chemotherapy, highly metastatic lesions (>3N⁺) or abundant CD45⁻ resident cells in mLN and high proportion of CD3⁺ at diagnosis in mLN favored the R phenotype in the adjuvant setting (Fig. S6d-f). mLN NK cells contrasted R from NR in neoadjuvant cases (Fig. S6g).

Altogether, redirecting polyclonal T cells to metastatic tumor cells, by connecting them via CD3 to a tumor-specific antigen on the surface of the LN tumor cell was efficient at triggering effector T (and indirectly NK) cell functions prior to chemotherapy in BC.

MHC class I loss in tumor-draining LN metastases

Three arguments point to a key role of tumor cells in triggering T cell reactivity in BC: i) the CD8/CD4 ratio of the mLN was positively correlated with the proportion of CD45⁻ cells (supposedly live residual tumor cells) (Fig. 1e), ii) the number of N⁺ and the proportion of CD45⁻ cells correlated with the efficacy of TCB (Fig. S6d-e), iii) chemotherapy did not pave the way to a better efficacy of TCB, suggesting that

elimination of tumor cells jeopardized the cross-linking of the target antigen with the CD3 ϵ (Fig. 2). Moreover, chemotherapy appeared to better target the primary lesions than the mLN by effectively reprogramming the TME while rendering mLN T cells more immunosuppressed (Tim3, Treg) (Fig. 1). These changes may account for the better efficacy of TCB in the mLN in adjuvant settings. Hence, we hypothesized that the density of the relevant MHC class I/ peptide complexes for the fitness of the T cell repertoire residing in mLN may be below the threshold of T cell reactivity. Immunohistochemistry staining of the specimen revealed a marked downregulation of MHC class I in 47 mLN compared to 52 primary BC, including 45 paired mLN/primary tumors (Fig. 4a-b left panel), across all molecular subtypes, including luminal cases for which TILs are not prognostic markers (Fig. 4c). Of note, about 1/3 of primary tumors harbored low/no MHC class I expression at diagnosis. Chemotherapy restored the MHC class I expression in distinct cases in mLN (Fig. 4b, right panel). Hence, other cases of HLA loss could be due to genetic deletions. Comparative genomic hybridization focusing on chromosome 6 and 15 where the loci of heavy chains of MHC class I molecules and the β 2 microglobulin (B2M) reside respectively, revealed genetic defects in B2M, more in metastatic (SAFIR01) than non-metastatic cohorts (TCGA) (Fig. 5a), and mostly in triple negative breast cancers, as assessed in SAFIR01 as well as in two distinct publicly available cohorts of primary BC (TCGA, METABRIC) (Fig. 5b).

To further investigate somatic loss of MHC class I molecules in primary tumor and mLN, we sequenced 9 tumor regions per patient (3 primary central, 3 primary peripheral, and 3 mLN) and a matched normal sample for 8 patients with luminal breast cancer according to a computational tool recently developed (17). We identified loss of heterozygosity of class I HLA alleles (HLA-LOH) in 5 out of 8 patients (62%; Fig. 5c). HLA LOH was subclonal in all five patients (Fig. 5d) with only HLA-A allele being subject to clonal LOH in one patient (Fig. 5c). Interestingly, we found a trend for enrichment for HLA loss in mLN as compared to central regions of the primary tumors (Fig. 5e-f, Table S5; two-sided *p*-value of Fisher's exact test 0.06).

We next characterized somatic MHC class I loss in the diagnostic core biopsy in a cohort of 154 patients treated with neo-adjuvant standard of care chemotherapy. 18% of cases had evidence of LOH of at least one

MHC class I allele prior to commencing chemotherapy, and tumors with presence of HLA LOH in the core biopsies were much less likely to have pathological complete response (OR 0.27; CI: 0.07-0.89, $p=0.04$, multiple logistic regression model factoring ER and HER2 status, Fig. 5g). In order to assess HLA abundance in the post-treatment samples, 24 cases were chosen based on their HLA LOH status at diagnosis (6 had evidence of HLA LOH) and presence of viable tumor tissue in both the primary breast tumor and metastatic lymph nodes. Following H-scoring, one sample was excluded as there were too few tumor cells in the breast tumor. In the 23 paired samples, there was a statistically significant decrease in H-score in the draining lymph nodes compared to breast tumor ($p=0.04$, Wilcoxon rank sum test), 12 samples showed a significant decrease while the other 11 samples showed no significant change (Fig.4b, neoadjuvant cases, $p=0.004$, Wilcoxon rank sum test in the paired analysis).

This observation showing the high frequency of genetic or non-genetic deficiencies in MHC class I expression in mLN further supports our hypothesis that metastatic lymph nodes are characterized by a lower density of MHC class I/peptide complexes than the primary BC tumors.

Discussion

The sentinel lymph node (SLN) is thought to be an important lymphoid organ for protecting against metastasis by eliciting anti-tumor immunity. However, our study unraveled, i) the profound immunosuppression residing in tumor-draining LN despite neoadjuvant chemotherapy supposed to reinstate local immuno-surveillance, ii) the capacity of TCB targeting CEACAM5 or HER2 to restore TILs effector functions despite low target antigen expression due to HLA-LOH.

The immunosuppressive microenvironment is a mainstay in BC, already detectable during the transition between *in situ* ductal carcinoma (DCIS) towards invasive BC (IDC). The CD8/Foxp3 ratio could be a hallmark of risk assessment for local recurrence and invasion in DCIS (18)(19). Our data show that neoadjuvant chemotherapy increased the proportion of Treg and Tim3 expression on CD4⁺ TILs in mLN while the CD8/CD4 ratio did not get ameliorated, in sharp contrast to what was observed in primary tumors.

The more immunosuppressive tumor environment of mLN (compared with the primary site) might be explained by the frequent loss of MHC class I molecules of the metastatic clones. Therefore, this study highlights the lack of effectiveness of conventional therapies to counteract natural immunosuppression mediated by BC progression to the first LN.

Importantly, bispecific T-cell engagers could restore T and NK cell functions in mLN (GrzB, Ki67, and IFN γ release in T cells), which are altered in IDC. Indeed, TILs gene products involved in TCR and cytokine receptor (IL-2RA and IL-10RA) signaling were upregulated in DCIS and normal breast compared with IDC (19). Moreover, DCIS CTLs harbored high clonal diversity in accordance with their high proliferative capacity and cytolytic pattern (19), features that are progressively lost in IDC. TCB tended to increase IL-2, IL-10, and CXCL10 (not shown) but did not increase inflammatory cytokines (Fig. 2, Fig3, Fig. S3) that are known to compromise TCR signaling by accelerating CD3 ζ degradation (20).

As an indirect argument supporting the relevance of T cells in BC immuno-surveillance, the emergence of antigen (MHC class I or proteins of the antigen processing machinery) loss variants has been described in HER2 positive BC, precluding proper recognition of HLA-A2-associated tumor epitopes by cytotoxic T cells (21). The proto-oncogene HER2 downregulates MHC class I expression through a RAS/Mitogen-activated protein kinase (MAPK)-dependent pathway (22). Likewise, chemotherapy and/or trastuzumab tend to eliminate HER2 overexpressing cells that are more sensitive to cytotoxic agents, paving the way to T cell responses, and the emergence of MHC class I loss variants. Several studies reported contradictory correlations between MHC class I loss and prognosis in BC (23)(24). MHC class I and II loss correlated with low MxA expression and fewer tertiary lymphoid structures and TILs in TNBC (25).

In advanced lung carcinomas, subclones harboring HLA-LOH were associated with a significantly elevated non-synonymous mutation/neoantigen burden and higher PD-L1 expression compared to subclones descended from the same ancestral tumor cell without HLA LOH (17). Using the same computational tool, we discovered a high prevalence (5/8 tumors) of HLA LOH in BC, suggesting HLA loss may be a pervasive mechanism of immune evasion in this cancer type as well, but at very early stages compared with lung tumors. Intriguingly, we found evidence for enrichment for HLA LOH in the lymph node metastasis (9/15

tumor samples) compared to central regions (3/15 tumor samples), suggesting HLA LOH may facilitate immune escape in the context of lymph node metastasis.

A considerable advantage of BiTE® or TCB molecules is that they directly engage any cytotoxic T cell and thus do not require the presence of preformed MHC class/peptide complexes, nor a high density of target antigens to mediate a full-blown T cell activation (10). Our study was biased towards probing novel therapeutic molecules onto available BC tissue samples that pathologists could provide after a comprehensive routine scoring of grade and tumor aggressiveness. Nonetheless, this bias enabled us to speculate that TCB could represent a reasonable alternative option to conventional chemotherapy (26). A related CEACAM5-T- cell bispecific (CEA-TCB, RO6958688, RG7802) antibody for the treatment of CEACAM5-expressing solid tumors currently in phase I clinical trials ([NCT02324257](https://clinicaltrials.gov/ct2/show/study/NCT02324257)), which led to encouraging results in advanced colorectal cancers. The high-avidity binding to CEACAM5 conferred by the antibody's design, together with the bivalent binding mode to tumor antigen, translates into an excellent therapeutic index, optimal efficacy with low toxicity profile (27).

Theoretically, TCB could eliminate MHC class I loss variants selected by chemotherapy, since our neoadjuvant trials indicated that HLA class I loss raised from 18% to 50% after 6 cycles. Indeed, TCB only improved CTL functions in mLN, and not in primary lesions (Fig. 2-3), because the latter ones are already partially triggered by immunogenic chemotherapy (Fig. S3). However, mLN could hardly be reactivated by TCB pre-exposed to chemotherapy, although chemotherapy did not ignite T cells in this case. Therefore, it may be more effective to reactivate preexisting tissue resident memory T cells (TRM) (28) using TCB upfront prior to surgery and/or chemotherapy to facilitate tumor killing and cross-presentation of novel tumor antigens for the creation of a new TCR repertoire, hence preventing additional MHC class I loss variants generated post-chemotherapy.

In fact, our data appear to indicate that the initial representativeness in CD8⁺ T cells together with high (>70%) invasion by CD45⁻ cells correlate with the TCB-mediated capacity to trigger proliferative and cytotoxic functions of effector cells and cytokine release in the TME, bypassing the HLA LOH associated with the immunosuppressive milieu. These findings warrant pilot trials in window-of-opportunity settings

before surgery and subsequent adjuvant chemotherapy to demonstrate the capacity of TCB to increase the CD8/CD4 ratio, GrzB on CD8⁺ T and NK cells and to decrease Ki67 in EpCAM⁺ tumor cells, not only in the primary tumor but most importantly in the metastatic LN.

Acknowledgements. We would like to thank, the Flow cytometry and Pathology Platforms of Gustave Roussy. We also would like to particularly thank Dr. Christian Klein, Dr. Vaios Karanikas, Dr. Pablo Umana from *Roche Pharmaceutical Research and Early Development, Translational Medicine Oncology Roche Innovation Center, Zurich, Switzerland.*

Funding. This work was supported by ROCHE, Institut National du Cancer (INCa), ANR, Ligue contre le cancer and Swiss Bridge Foundation, ISREC Foundation, LABEX OncoImmunology, la direction generale de l'offre de soins (DGOS), Universite Paris-Sud, SIRIC SOCRATE (INCa/DGOS/INSERM 6043), and PIA2 TORINO-LUMIERE.

Competing interests. The authors declare no competing interests.

References :

1. Salgado R, Denkert C, Demaria S, et al. The evaluation of tumor-infiltrating lymphocytes (TILs) in breast cancer: recommendations by an International TILs Working Group 2014. *Ann Oncol Off J Eur Soc Med Oncol.* 2015 Feb;26(2):259–71.
2. Loi S, Sirtaine N, Piette F, et al. Prognostic and predictive value of tumor-infiltrating lymphocytes in a phase III randomized adjuvant breast cancer trial in node-positive breast cancer comparing the addition of docetaxel to doxorubicin with doxorubicin-based chemotherapy: BIG 02-98. *J Clin Oncol Off J Am Soc Clin Oncol.* 2013 Mar 1;31(7):860–7.
3. Liu S, Lachapelle J, Leung S, et al. CD8⁺ lymphocyte infiltration is an independent favorable prognostic indicator in basal-like breast cancer. *Breast Cancer Res BCR.* 2012 Mar 15;14(2):R48.
4. Kroemer G, Senovilla L, Galluzzi L, André F, Zitvogel L. Natural and therapy-induced immunosurveillance in breast cancer. *Nat Med.* 2015 Oct;21(10):1128–38.
5. Galluzzi L, Buqué A, Kepp O, Zitvogel L, Kroemer G. Immunological Effects of Conventional Chemotherapy and Targeted Anticancer Agents. *Cancer Cell.* 2015 Dec 14;28(6):690–714.
6. Haricharan S, Bainbridge MN, Scheet P, Brown PH. Somatic mutation load of estrogen receptor-positive

breast tumors predicts overall survival: an analysis of genome sequence data. *Breast Cancer Res Treat*. 2014 Jul;146(1):211–20.

7. Miles D, Roché H, Martin M, et al. Phase III multicenter clinical trial of the sialyl-TN (STn)-keyhole limpet hemocyanin (KLH) vaccine for metastatic breast cancer. *The Oncologist*. 2011;16(8):1092–100.

8. Nanda R, Chow LQM, Dees EC, et al. Pembrolizumab in Patients With Advanced Triple-Negative Breast Cancer: Phase Ib KEYNOTE-012 Study. *J Clin Oncol Off J Am Soc Clin Oncol*. 2016 Jul 20;34(21):2460–7.

9. Schmid P, Adams S, Rugo HS, et al. Atezolizumab and Nab-Paclitaxel in Advanced Triple-Negative Breast Cancer. *N Engl J Med*. 2018 Nov 29;379(22):2108–21.

10. Baeuerle PA, Reinhardt C. Bispecific T-cell engaging antibodies for cancer therapy. *Cancer Res*. 2009 Jun 15;69(12):4941–4.

11. Mack M, Riethmüller G, Kufer P. A small bispecific antibody construct expressed as a functional single-chain molecule with high tumor cell cytotoxicity. *Proc Natl Acad Sci U S A*. 1995 Jul 18;92(15):7021–5.

12. Bacac M, Fauti T, Sam J, et al. A Novel Carcinoembryonic Antigen T-Cell Bispecific Antibody (CEA TCB) for the Treatment of Solid Tumors. *Clin Cancer Res Off J Am Assoc Cancer Res*. 2016 Jul 1;22(13):3286–97.

13. André F, Bachelot T, Commo F, et al. Comparative genomic hybridisation array and DNA sequencing to direct treatment of metastatic breast cancer: a multicentre, prospective trial (SAFIR01/UNICANCER). *Lancet Oncol*. 2014 Mar;15(3):267–74.

14. Jacquelot N, Roberti MP, Enot DP, Rusakiewicz S, Ternès N, Jegou S, et al. Predictors of responses to immune checkpoint blockade in advanced melanoma. *Nat Commun*. 2017 Sep 19;8(1):592.

15. Commo F, Guinney J, Ferté C, et al. rCGH: a comprehensive array-based genomic profile platform for precision medicine. *Bioinforma Oxf Engl*. 2016 May 1;32(9):1402–4.

16. Bacac M, Klein C, Umana P. CEA TCB: A novel head-to-tail 2:1 T cell bispecific antibody for treatment of CEA-positive solid tumors. *Oncoimmunology*. 2016 Aug;5(8):e1203498.

17. McGranahan N, Rosenthal R, Hiley CT, et al. Allele-Specific HLA Loss and Immune Escape in Lung Cancer Evolution. *Cell*. 2017 Nov 30;171(6):1259–1271.e11.

18. Semeraro M, Adam J, Stoll G, et al. The ratio of CD8(+)/FOXP3 T lymphocytes infiltrating breast tissues predicts the relapse of ductal carcinoma in situ. *Oncoimmunology*. 2016;5(10):e1218106.

19. Gil Del Alcazar CR, Huh SJ, Ekram MB, et al. Immune Escape in Breast Cancer During In Situ to Invasive Carcinoma Transition. *Cancer Discov*. 2017 Oct;7(10):1098–1115.

20. Érsek B, Molnár V, Balogh A, et al. CD3ζ-chain expression of human T lymphocytes is regulated by TNF via Src-like adaptor protein-dependent proteasomal degradation. *J Immunol Baltim Md 1950*. 2012 Aug 15;189(4):1602–10.

21. Mimura K, Ando T, Poschke I, et al. T cell recognition of HLA-A2 restricted tumor antigens is impaired by the oncogene HER2. *Int J Cancer*. 2011 Jan 15;128(2):390–401.

22. Inoue M, Mimura K, Izawa S, et al. Expression of MHC Class I on breast cancer cells correlates inversely with HER2 expression. *Oncoimmunology*. 2012 Oct 1;1(7):1104–10.

23. Madjd Z, Spendlove I, Pinder SE, Ellis IO, Durrant LG. Total loss of MHC class I is an independent indicator of good prognosis in breast cancer. *Int J Cancer*. 2005 Nov 1;117(2):248–55.

24. Kaneko K, Ishigami S, Kijima Y, et al. Clinical implication of HLA class I expression in breast cancer. *BMC Cancer*. 2011 Oct 20;11:454.
25. Lee HJ, Song IH, Park IA, et al. Differential expression of major histocompatibility complex class I in subtypes of breast cancer is associated with estrogen receptor and interferon signaling. *Oncotarget*. 2016 May 24;7(21):30119–32.
26. Klein C, Schaefer W, Regula JT. The use of CrossMAb technology for the generation of bi- and multispecific antibodies. *mAbs*. 2016 Sep;8(6):1010–20.
27. Argilés G, Saro J, Segal NH, et al. LBA-004 Novel carcinoembryonic antigen T-cell bispecific (CEA-TCB) antibody: Preliminary clinical data as a single agent and in combination with atezolizumab in patients with metastatic colorectal cancer (mCRC). *Ann Oncol Off J Eur Soc Med Oncol*. 2017 Jun 1;28(suppl_3).
28. Savas P, Virassamy B, Ye C, et al. Single-cell profiling of breast cancer T cells reveals a tissue-resident memory subset associated with improved prognosis. *Nat Med*. 2018 Jul;24(7):986–93.

Figure Legends

Figure 1. Regulatory T cells and Tim3 expression in BC metastatic lymph nodes (mLN) despite immunogenic chemotherapy.

a. Relative percentages of the whole CD8⁺ cell fraction among live CD3⁺ cells and of the granzyme B expressing cells in the gate of CD8⁺ T cells. **b.** Ratio of CD8/CD4 tumor infiltrating T lymphocytes (TILs) in all 4 settings. **c.** Expression of distinct immune checkpoints on CD4⁺ T cells from primary tumor BC or mLN. **d.** Fraction of CD45⁻ cells remaining alive after dissociation. **e.** Spearman correlations between CD45⁻ cells and the ratio of CD8/CD4 in TILs in primary tumor versus mLN in the adjuvant and neoadjuvant settings. The number of specimen is annotated. Unpaired Mann-Whitney t'test: * $p < 0.05$, ** $p < 0.01$, *** $p < 0.001$.

Figure 2. Metastatic lymph nodes respond to HER2 targeted-T (HER2-T) cell bispecific antibodies.

a. Heatmap depicting the biological effects of HER2-T in mLN and primary tumors over controls in adjuvant settings performed at Day 1 (grey color: ND). **b-e.** T (b, d, e) and NK (c) functions investigated prior to chemotherapy using flow cytometry after intracellular staining, gating on live CD45⁺ cell fraction of dissociated primary BC or mLN. Relative percentages of granzyme B expressing CD8⁺ T and NK cells (b, c) at Day 1 or Day 6. **d.** Relative percentages of proliferative (% Ki67⁺) CD8⁺ T or NK cells (at Day 6). **e.** IFN γ -expressing CD8⁺ or CD4⁺ T cells tested at Day 1. Each dot represents one specimen and lines represent means of all dots. The number of specimen is annotated for each conditions: medium, versus isotype control mAb [Ctrl-T (isotype control for the HER2-T), HER2-T or recombinant human IL-2 (rIL-2). ND: Not determined. Unpaired Mann-Whitney t'test: * $p < 0.05$, ** $p < 0.01$, or indicated p -value for trends. Also refer to Fig. S3-4 for comprehensive analyses of immune parameters in neoadjuvant settings and dose effects.

Figure 3. Metastatic lymph nodes respond to CEACAM5 targeted-T cell bispecific antibodies (CEACAM5-T).

T and NK cell functions in primary BC and mLN assessed after dissociation and incubation with CEACAM5-T at increasing dosing, prior to adjuvant chemotherapy monitored by flow cytometry after intracellular staining. **a.** Heat-maps depicting the biological effects of CEACAM5-T in mLN and primary tumors over controls in adjuvant settings performed at Day 1 and Day 6 (grey color: ND). **b-c.** Relative percentages of granzyme B, Ki67 or IFN γ expressing CD8⁺ T cells (at Day 1 or Day 6) (b) or NK cells (c). Each dot represents one specimen and lines represent means of all dots. The number of specimen is annotated for each condition: medium, versus isotype control mAb [Ctrl-T (isotype control for the CEACAM5-T), CEACAM5-T or recombinant human IL-2 (rIL-2), as outlined. **d.** Pooled data from all 10 specimen segregated according to values >10% positivity, in control (medium, Ctrl-T) versus TCB exposed wells. Chi-square test and Unpaired Mann-Whitney t'test: * p <0.05, ** p <0.01.

Figure 4. Diagnosis of MHC class I deficiency in early BC by immunohistochemistry.

a. Representative micrograph pictures of IHC stainings using anti-HLA ABC mAb on paired primary and mLN BC at different magnitudes. **b-c.** H-score of MHC class I expression using anti-HLA ABC antibody in primary and mLN from BC, segregating the BC cases according to adjuvant versus neoadjuvant settings and the molecular subtyping. The paired cases are linked with a line. Paired Wilcoxon statistics: * p <0.05, ** p <0.01, *** p <0.001.

Figure 5. Subclonal HLA LOH in early BC.

a-b. Loss of *B2M* in metastatic BC. CGH array of $N=695$ metastatic lesions (SAFIR01) compared with TCGA and METABRIC cohorts ($N=1080$), analyzing chromosome 6 and 15 associated-MHC loci. **c.** Percentage of BC patients ($N=8$) harboring (orange) or not (grey) HLA LOH as measured by HLA LOH and allele-specific characterization of clonal (red) and subclonal (purple) status. **d.** Number of BC patients

with matched primary tumor and lymph node metastasis exhibiting no HLA LOH (grey), HLA LOH in both primary tumor and lymph nodes (green), HLA LOH in primary tumor only (blue) and HLA LOH in metastatic lymph nodes only (magenta). **e.** Percentage of regions harboring HLA LOH for central, peripheral and lymph node metastases. Analysis was performed for the 5 patients identified with HLA LOH. **f.** Representative example of the Log Ratio calculated in HLA LOH from a peripheral and a metastatic lymph node sample of a BC patient with HLA LOH. Open circles represent mismatch positions between the two HLA alleles. **g.** HLA LOH status and association with response to chemotherapy.

Supplementary materials.

Supplementary Figure 1. Breast cancers harbour an immunosuppressive milieu compared with surrounding healthy tissues (HT).

Flow cytometric analyses of different immune subsets gating on the live CD45⁺ cell fraction of dissociated primary breast cancers or surrounding “healthy” tissues (HT) in a paired fashion (linked dots) or not (a-c).

a. Relative percentages of the whole CD45⁺ cell fraction among live cells. **b.** Percentages of CD25^{high}CD127^{low} regulatory T cells among CD3⁺CD4⁺ T lymphocytes (left panel) in all BC or according to different molecular subtypes (right panel). **c.** Proportion of CD3⁺CD4⁺ T cells or CD3⁺CD8⁺ T cells coexpressing PD-1 and PD-L1 in paired HT or BC (left and middle panels) and percentages of PD-L1 expressing non T non NK cells (CD3⁻CD56⁻ cells) among live CD45⁺ cells (right panel). The number of specimen is annotated. *Wilcoxon statistics: *p<0.05, **p<0.01. Also refer to Table S4 depicting comprehensive analyses of immune parameters in all three BC molecular subtypes.

Supplementary Figure 2. Experimental setting of the « *ex vivo* mLN assay ».

Primary BC or metastatic lymph nodes (mLN) (composed of 0.1-99% of CD45 negative cells) were resected, and freshly mechanically and enzymatically dissociated using the Miltenyi Gentle MACS

equipment for 1 hour at 37°C under rotation (2 incubation steps of 30 minutes). Whole cell suspensions were incubated in duplicate wells (one for the 18-24h readout and one for the 6 days readout) at 0.25×10^6 /ml with medium, versus isotype control mAb [untargeted-T= Ctrl-T (isotype control for the HER2-T and CEACAM5-T), DP47 (isotype control for anti-FAP-4-1BBL)] or a series of TCB or bispecific agonistic mAbs, combinations, or recombinant human IL-2 (rIL-2), as outlined. For the conditions 17, 18, 19 and 20, two phase-process: 24h with HER2-T followed from Day 1 to Day 6 by stimulation with anti-FAP-4-1BBL or its Isotype control DP47. The *ex vivo* stimulation lasted 18-24h before flow cytometric analyses of live CD45⁺ cells, or gated within CD3⁺CD4⁺, CD3⁺CD8⁺, or CD3⁺CD56⁺ cells for intracellular staining of Th1 cytokines (IFN γ , TNF α) after a final 5hr activation with PMA/Ionomycin and GolgiStop. The 18-24hr cytokine release was monitored by commercial ELISA. The Day 6 time point was crucial for monitoring proliferation, based on Ki67 expression assessed by flow cytometric analyses on T, NK, and Treg populations.

Supplementary Figure 3. Heat-maps depicting the biological effects of HER2-T in mLN and primary lesions over controls in neoadjuvant settings.

a. Heat-map depicting the immunometrics scoring over isotype control antibodies after HER2-T in neoadjuvant BC performed at Day 1 (left panel) and Day 6 (right panel). All assays have been run in duplicate wells. Each column represents a patient/lesion and each row a parameter (an immunometric). Grey cells indicate that the marker could not be evaluated for the corresponding patient. **b.** Relative percentages of granzyme B expressing cells in the gate of CD8⁺ T cells and **c.** in the gate of NK cells (b, c) at Day 1. **d.** Relative percentages of proliferative (% Ki67⁺) CD8⁺ T cells or NK cells (at Day 6). **e.** IFN γ ⁺ expressing CD8⁺ or CD4⁺ T cells tested at Day 1. Each dot represents one specimen/patient and lines represent means of all dots. The number of specimen is annotated for each condition: medium, versus isotype control mAb [untargeted-T, Ctrl-T (isotype control for the HER2-T), HER2-T or recombinant human IL-2 (rIL-2), as outlined. *ND*: Not determined. Unpaired Mann-Whitney t'test were assessed.

Supplementary Figure 4. Dose effect of HER2-T on metastatic lymph nodes.

Relative percentages of GrzB at Day 1 in CD8⁺ T cells in tumor or mLN incubated with increasing doses of HER2-T and its untargeted controls (Ctrl-T) (process detailed in Fig. S2) during adjuvant and neoadjuvant chemotherapy settings. Graph bars representing means of duplicate wells for at least 3 lesions.

Supplementary Figure 5. Combination of T Cell Bispecific (TCB) Antibodies with next generation immune-targeted antibodies.

a, b. Relative percentages of GrzB expressing CD8⁺ T cells and NK cells after CEACAM5-T or HER2-T in two patients. **c, d, e.** Flow cytometric determination of Tim3, CD137L (4-1-BBL) and FAP expression by tumor (CD45⁻) or CD4⁺ and CD8⁺ T cells at Day 1 of stimulation with HER2-T or other reagents in different patients' lesions. **f-h.** Data from 34 lesions showing Th1 cytokine producing T cells; GrzB and Ki67 expressing CD8⁺ T cells and NK cells incubated with HER2-T for 24hrs followed by anti-FAP-4-1BBL antibody. The percentages of flow cytometric measures were normalized to medium alone. The values represent the means of two wells. Only one experiment could be performed on one single lesion per patient precluding valid statistical analyses.

Supplementary Figure 6. Predictors of response to T cell Bispecific (TCB) Antibodies.

Responsiveness (R) was defined as co-cultures leading to 3 concomitant positive readouts after exposure to either one of the two TCB (among Granzyme B (GrzB), and/or Ki67, in CD4⁺T, and/or CD8⁺ T and/or NK cells, 1.5-fold increase over the medium and isotype control (Ctrl-T) Abs was scored "R" as defined in (14)). Resistance (Non responder, NR) encompassed all the other cases. **a-b.** Associations between H-score (established in IHC by pathologists) for HER2 and responsiveness to the HER2-T for R versus NR status (a) and also considering % CD8⁺GrzB⁺ at Day 1 criteriums. **c.** Associations between H-score (established in IHC by pathologists) for CEACAM5 and responsiveness to the CEACAM5-T for R versus NR status in ten lesions in adjuvant setting. HER2 expression levels by tumor cells (as defined by

semi-quantitative IHC score and not by FISH analyses) allowed contrasting R from NR lesions. CEACAM5 expression levels were also defined by IHC H-score in tested lesions ($N=10$) studied in adjuvant setting, the negative CEACAM5 lesions (H-score=0) were NR (c, left panel), while 5/8 expressing lesions (H-score>0) were R (c, right panel). **d-e.** Correlation between R/NR phenotype and the number of invaded LN (c) or flow cytometry determination of % CD45- cells (d). **f.** Spearman correlation between the proportion of CD3⁺ cells at diagnosis and responsiveness to TCB on this parameter. **g-i.** Associations between the proportion of NK (g) cells, Tim3 and PD1 (h, i) expression on T cells at diagnosis and responsiveness to TCB in adjuvant and neoadjuvant settings analyzed in Fig. 1-2 and presented in Table S1-2. Each dot represents one specimen/patient and lines represent means of all dots. The number of specimen is annotated. Unpaired Mann-Whitney t'test: * $p<0.05$, ** $p<0.01$.

Supplementary Table 1. Patient and Tumor Characteristics in the adjuvant cohort.

Supplementary Table 2. Patient and Tumor Characteristics in the Neoadjuvant Cohort.

Supplementary Table 3. List of fluorochrome-coupled mAbs for flow cytometry.

Supplementary Table 4. Immune profiling in HR+, HER2 and TNBC.

Supplementary Table 5. Summary of HLA LOH identified in 5 breast cancer patients. For each tumour region in each patient, the location of the region (i.e peripheral, central or lymph node), the region's name, the HLA genotype, the LOH HLA copy number and p -value are reported.

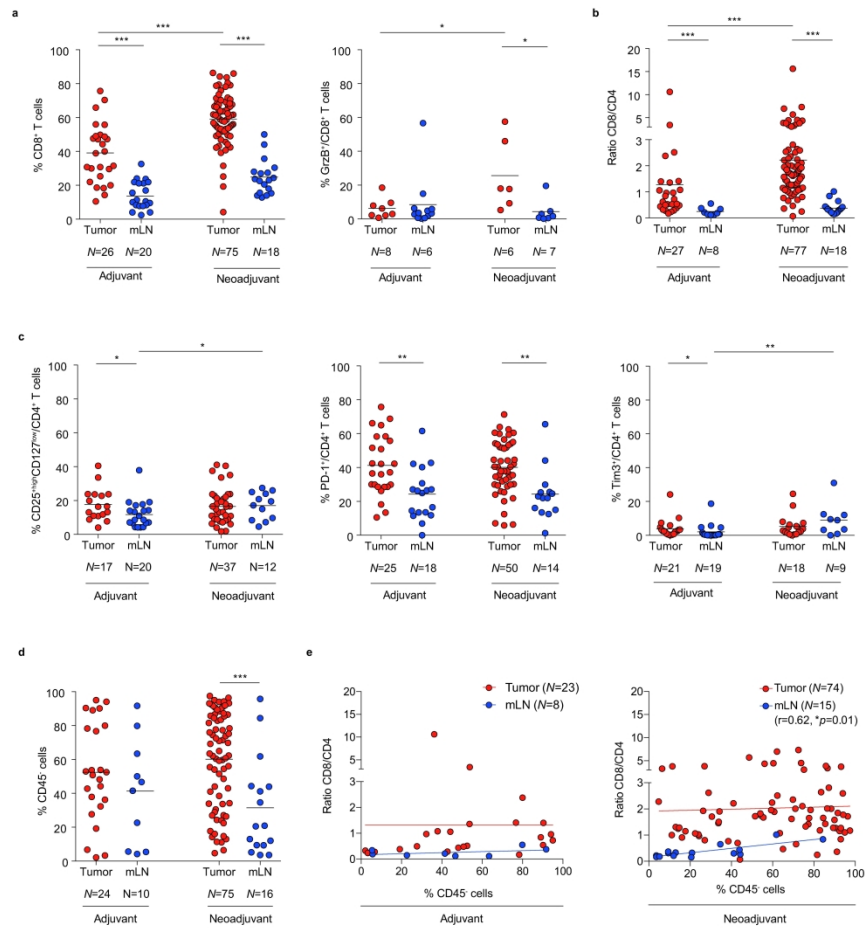


Figure 1

Figure 1. Regulatory T cells and Tim3 expression in BC metastatic lymph nodes (mLN) despite immunogenic chemotherapy.

a. Relative percentages of the whole CD8⁺ cell fraction among live CD3⁺ cells and of the granzyme B expressing cells in the gate of CD8⁺ T cells in all 4 settings. b. Ratio of CD8/CD4 tumor infiltrating T lymphocytes (TILs) in all 4 settings. c. Expression of distinct immune checkpoints on CD4⁺ T cells from primary tumor BC or mLN. d. Fraction of CD45⁻ cells remaining alive after dissociation. e. Spearman correlations between CD45⁻ cells and the ratio of CD8/CD4 in TILs in primary tumor versus mLN in the adjuvant and neoadjuvant settings. The number of specimen is annotated. Unpaired Mann-Whitney t-test: * $p < 0.05$, ** $p < 0.01$, *** $p < 0.001$.

293x412mm (300 x 300 DPI)

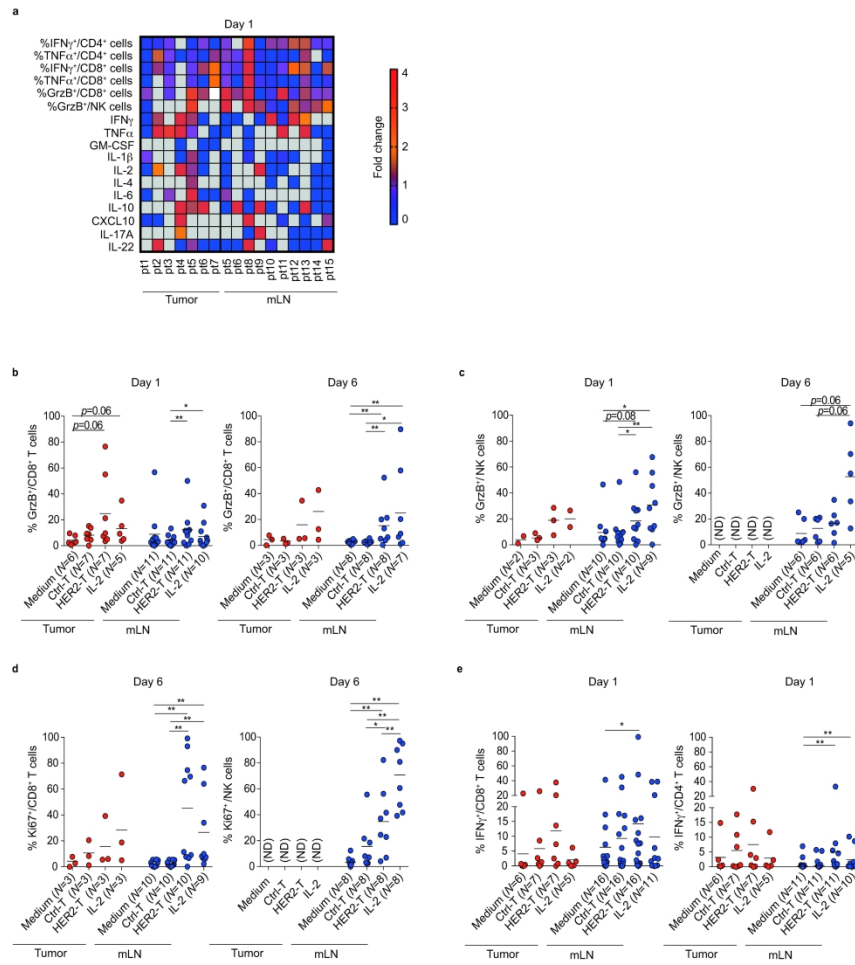


Figure 2

Figure 2. Metastatic lymph nodes respond to HER2 targeted-T (HER2-T) cell bispecific antibodies. a. Heatmap depicting the biological effects of HER2-T in mLN and primary tumors over controls in adjuvant settings performed at Day 1 (grey color: ND). b-e. T (b, d, e) and NK (c) functions investigated prior to chemotherapy using flow cytometry after intracellular staining, gating on live CD45+ cell fraction of dissociated primary BC or mLN. Relative percentages of granzyme B expressing CD8+ T and NK cells (b, c) at Day 1 or Day 6. d. Relative percentages of proliferative (% Ki67+) CD8+ T or NK cells (at Day 6). e. IFN γ expressing CD8+ or CD4+ T cells tested at Day 1. Each dot represents one specimen and lines represent means of all dots. The number of specimen is annotated for each conditions: medium, versus isotype control mAb Ctrl-T (isotype control for the HER2-T), HER2-T or recombinant human IL-2 (rIL-2). ND: Not determined. Unpaired Mann-Whitney t-test: * $p < 0.05$, ** $p < 0.01$, or indicated p-value for trends. Also refer to Fig. S3-4 for comprehensive analyses of immune parameters in neoadjuvant settings and dose effects.

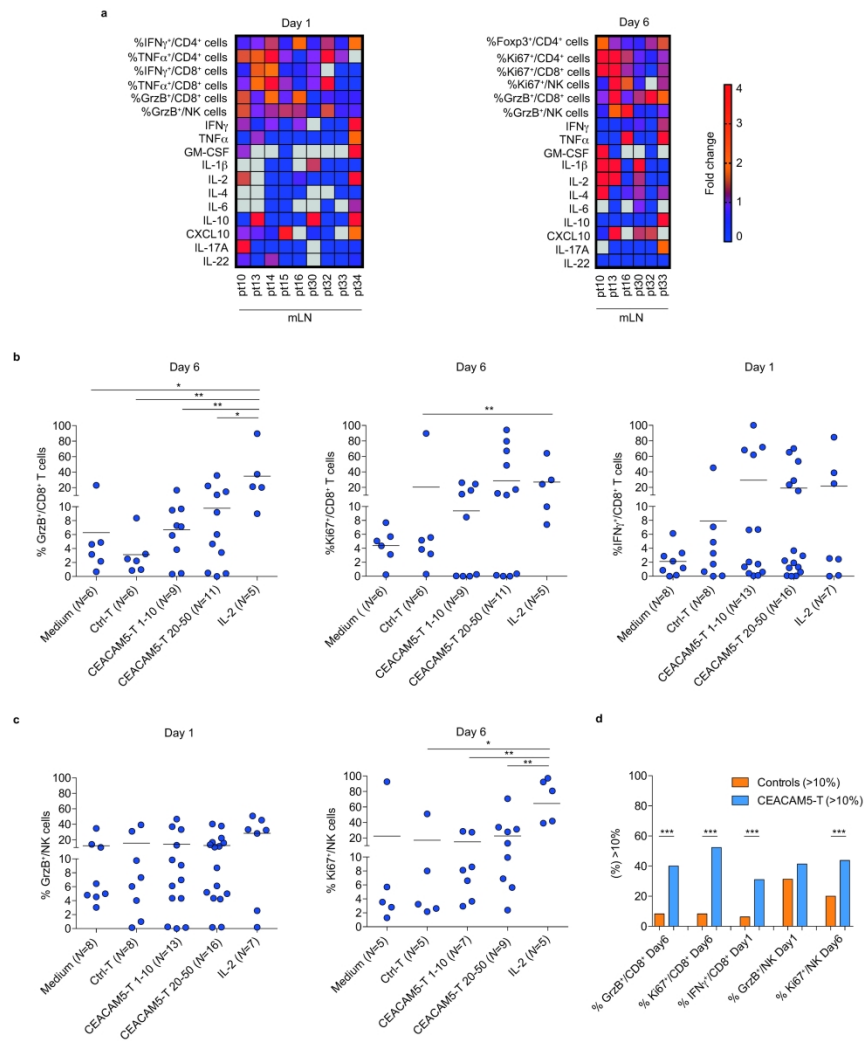


Figure 3

Figure 3. Metastatic lymph nodes respond to CEACAM5 targeted-T cell bispecific antibodies (CEACAM5-T). T and NK cell functions in primary BC and mLN assessed after dissociation and incubation with CEACAM5-T at increasing dosing, prior to adjuvant chemotherapy monitored by flow cytometry after intracellular staining. a. Heat-maps depicting the biological effects of CEACAM5-T in mLN and primary tumors over controls in adjuvant settings performed at Day 1 and Day 6 (grey color: ND). b-c. Relative percentages of granzyme B, Ki67 or IFN γ expressing CD8 $^+$ T cells (at Day 1 or Day 6) (b) or NK cells (c). Each dot represents one specimen and lines represent means of all dots. The number of specimen is annotated for each condition: medium, versus isotype control mAb Ctrl-T (isotype control for the CEACAM5-T), CEACAM5-T or recombinant human IL-2 (rIL-2), as outlined. d. Pooled data from all 10 specimen segregated according to values >10% positivity, in control (medium, Ctrl-T) versus TCB exposed wells. Chi-square test and Unpaired Mann-Whitney t-test: * p <0.05, ** p <0.01.

287x404mm (300 x 300 DPI)

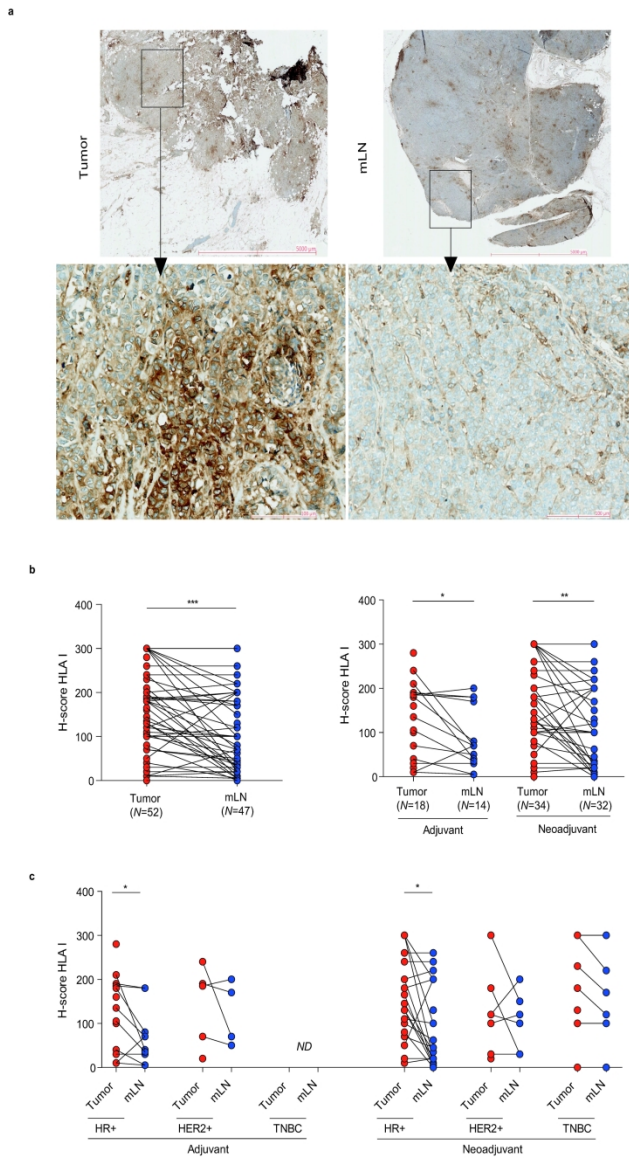


Figure 4

Figure 4. Diagnosis of MHC class I deficiency in early BC by immunohistochemistry. a. Representative micrograph pictures of IHC stainings using anti-HLA ABC mAb on paired primary and mLN BC at different magnitudes. b-c. H-score of MHC class I expression using anti-HLA ABC antibody in primary and mLN from BC, segregating the BC cases according to adjuvant versus neoadjuvant settings and the molecular subtyping. The paired cases are linked with a line. Paired Wilcoxon statistics: *p<0.05, **p<0.01, ***p<0.001.

254x403mm (300 x 300 DPI)

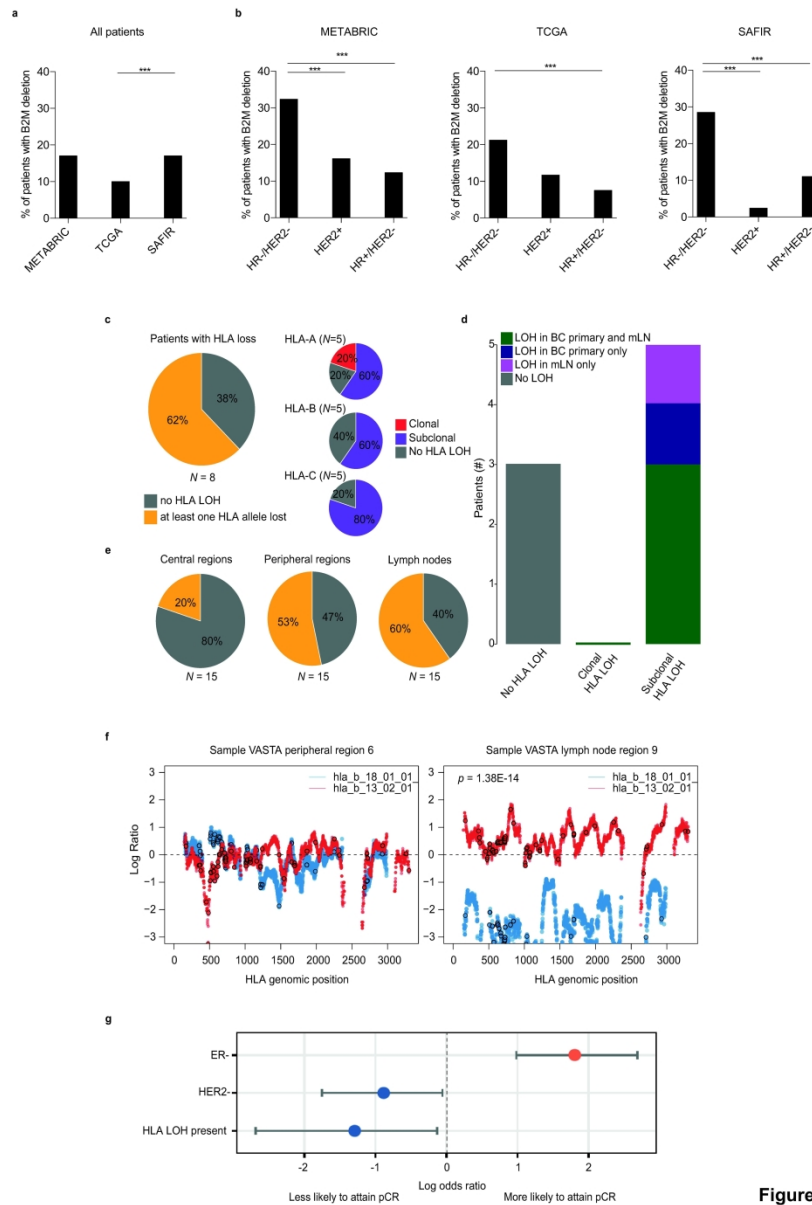


Figure 5

Figure 5. Subclonal HLA LOH in early BC.

a-b. Loss of B2M in metastatic BC. CGH array of N=695 metastatic lesions (SAFIR01) compared with TCGA and METABRIC cohorts (N=1080), analyzing chromosome 6 and 15 associated-MHC loci. c. Percentage of BC patients (N=8) harboring (orange) or not (grey) HLA LOH as measured by HLA LOH and allele-specific characterization of clonal (red) and subclonal (purple) status. d. Number of BC patients with matched primary tumor and lymph node metastasis exhibiting no HLA LOH (grey), HLA LOH in both primary tumor and lymph nodes (green), HLA LOH in primary tumor only (blue) and HLA LOH in metastatic lymph nodes only (magenta). e. Percentage of regions harboring HLA LOH for central, peripheral and lymph node metastases. Analysis was performed for the 5 patients identified with HLA LOH. f. Representative example of the Log Ratio calculated in HLA LOH from a peripheral and a metastatic lymph node sample of a BC patient with HLA LOH. Open circles represent mismatch positions between the two HLA alleles. g. HLA LOH status and association with response to chemotherapy.

283x414mm (300 x 300 DPI)